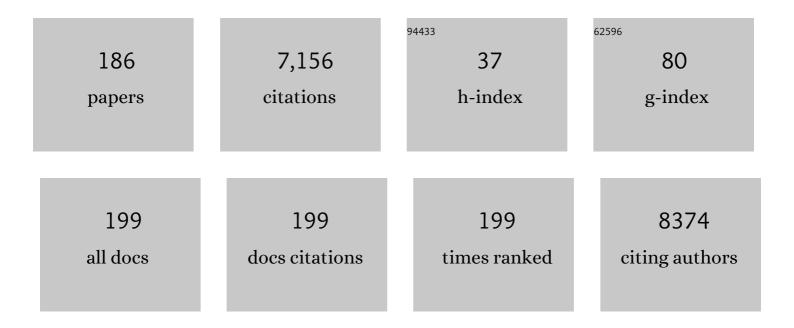
Pierre Croisille

List of Publications by Year in descending order

Source: https://exaly.com/author-pdf/9105399/publications.pdf Version: 2024-02-01



#	Article	IF	CITATIONS
1	Effect of Cyclosporine on Reperfusion Injury in Acute Myocardial Infarction. New England Journal of Medicine, 2008, 359, 473-481.	27.0	1,189
2	Assessment of Myocardial Fibrosis With Cardiovascular Magnetic Resonance. Journal of the American College of Cardiology, 2011, 57, 891-903.	2.8	802
3	Physiological Basis of Myocardial Contrast Enhancement in Fast Magnetic Resonance Images of 2-Day-Old Reperfused Canine Infarcts. Circulation, 1995, 92, 1902-1910.	1.6	390
4	Cardiac MRI Endpoints in MyocardialÂInfarction Experimental andÂClinicalÂTrials. Journal of the American College of Cardiology, 2019, 74, 238-256.	2.8	235
5	Human Atlas of the Cardiac Fiber Architecture: Study on a Healthy Population. IEEE Transactions on Medical Imaging, 2012, 31, 1436-1447.	8.9	201
6	Post-Conditioning Reduces Infarct Size and Edema in Patients With ST-Segment Elevation Myocardial Infarction. Journal of the American College of Cardiology, 2012, 59, 2175-2181.	2.8	194
7	Diastolic Dysfunction in Patients with Type 2 Diabetes Mellitus: Is It Really the First Marker of Diabetic Cardiomyopathy?. Journal of the American Society of Echocardiography, 2011, 24, 1268-1275.e1.	2.8	190
8	Effect of Cyclosporine on Left Ventricular Remodeling After Reperfused Myocardial Infarction. Journal of the American College of Cardiology, 2010, 55, 1200-1205.	2.8	170
9	Intracoronary autologous mononucleated bone marrow cell infusion for acute myocardial infarction: results of the randomized multicenter BONAMI trial. European Heart Journal, 2011, 32, 1748-1757.	2.2	158
10	Impaired Myocardial Radial Function in Asymptomatic Patients with Type 2 Diabetes Mellitus: A Speckle-Tracking Imaging Study. Journal of the American Society of Echocardiography, 2010, 23, 1266-1272.	2.8	136
11	Prognostic Value of Routine Cardiac Magnetic Resonance Assessment of Left Ventricular Ejection Fraction and Myocardial Damage. Circulation: Cardiovascular Imaging, 2011, 4, 610-619.	2.6	119
12	Myocardial Tagging with MR Imaging: Overview of Normal and Pathologic Findings. Radiographics, 2012, 32, 1381-1398.	3.3	105
13	Longitudinal Myocardial Strain Alteration Is Associated with Left Ventricular Remodeling in Asymptomatic Patients with Type 2 Diabetes Mellitus. Journal of the American Society of Echocardiography, 2014, 27, 479-488.	2.8	96
14	Controversies in Cardiovascular MR Imaging: T2-weighted Imaging Should Not Be Used to Delineate the Area at Risk in Ischemic Myocardial Injury. Radiology, 2012, 265, 12-22.	7.3	91
15	Cardiac and respiratory double self-gated cine MRI in the mouse at 7 T. Magnetic Resonance in Medicine, 2006, 55, 506-513.	3.0	88
16	Differentiation of Viable and Nonviable Myocardium by the Use of Three-Dimensional Tagged MRI in 2-Day-Old Reperfused Canine Infarcts. Circulation, 1999, 99, 284-291.	1.6	84
17	Postconditioning attenuates no-reflow in STEMI patients. Basic Research in Cardiology, 2013, 108, 383.	5.9	81
18	Effect of Colchicine on Myocardial Injury in Acute Myocardial Infarction. Circulation, 2021, 144, 859-869	1.6	74

#	Article	IF	CITATIONS
19	Pulmonary nodules: improved detection with vascular segmentation and extraction with spiral CT. Work in progress Radiology, 1995, 197, 397-401.	7.3	72
20	Shear-Wave Elastography Assessments of Quadriceps Stiffness Changes prior to, during and after Prolonged Exercise: A Longitudinal Study during an Extreme Mountain Ultra-Marathon. PLoS ONE, 2016, 11, e0161855.	2.5	71
21	Comparison of Immediate With Delayed Stenting Using the Minimalist Immediate Mechanical Intervention Approach in Acute ST-Segment–Elevation Myocardial Infarction. Circulation: Cardiovascular Interventions, 2016, 9, e003388.	3.9	71
22	Automated myocardial edge detection from breath-hold cine-MR images: Evaluation of left ventricular volumes and mass. Magnetic Resonance Imaging, 1994, 12, 589-598.	1.8	69
23	Airway Narrowing in Healthy Humans Inhaling Methacholine without Deep Inspirations Demonstrated by HRCT. American Journal of Respiratory and Critical Care Medicine, 2000, 161, 1256-1263.	5.6	61
24	Contrast agents and cardiac MR imaging of myocardial ischemia: from bench to bedside. European Radiology, 2006, 16, 1951-1963.	4.5	60
25	Determination of the myocardial area at risk with pre- versus post-reperfusion imaging techniques in the pig model. Basic Research in Cardiology, 2011, 106, 1247-1257.	5.9	58
26	Subclinical diastolic dysfunction in young adults with Type 2 diabetes mellitus: a multiparametric contrast-enhanced cardiovascular magnetic resonance pilot study assessing potential mechanisms. European Heart Journal Cardiovascular Imaging, 2014, 15, 1263-1269.	1.2	58
27	Myocardial Extracellular Volume Estimation by CMR Predicts Functional Recovery Following Acute Ml. JACC: Cardiovascular Imaging, 2017, 10, 989-999.	5.3	57
28	Two-dimensional spatial and temporal displacement and deformation field fitting from cardiac magnetic resonance tagging. Medical Image Analysis, 2000, 4, 253-268.	11.6	55
29	Evaluation of Peak Wall Stress in an Ascending Thoracic Aortic Aneurysm Using FSI Simulations: Effects of Aortic Stiffness and Peripheral Resistance. Cardiovascular Engineering and Technology, 2018, 9, 707-722.	1.6	54
30	Quantification of Myocardial Extracellular Volume Fraction with Cardiac MR Imaging for Early Detection of Left Ventricle Involvement in Systemic Sclerosis. Radiology, 2014, 271, 373-380.	7.3	49
31	In Vivo Cardiac Diffusion-Weighted Magnetic Resonance Imaging. Investigative Radiology, 2012, 47, 662-670.	6.2	48
32	Low b-Value Diffusion-Weighted Cardiac Magnetic Resonance Imaging. Investigative Radiology, 2011, 46, 751-758.	6.2	44
33	In vivo freeâ€breathing DTI and IVIM of the whole human heart using a realâ€time sliceâ€followed SEâ€EPI navigatorâ€based sequence: A reproducibility study in healthy volunteers. Magnetic Resonance in Medicine, 2016, 76, 70-82.	3.0	43
34	Systolic Myocardial Dysfunction in Patients with Type 2 Diabetes Mellitus: Identification at MR Imaging with Cine Displacement Encoding with Stimulated Echoes. Radiology, 2012, 265, 402-409.	7.3	42
35	Fluid- and Biomechanical Analysis of Ascending Thoracic Aorta Aneurysm with Concomitant Aortic Insufficiency. Annals of Biomedical Engineering, 2017, 45, 2921-2932.	2.5	42
36	Imaging Interstitial Fibrosis, LeftÂVentricular Remodeling, and Function in Stage A and B HeartÂFailure. JACC: Cardiovascular Imaging, 2021, 14, 1038-1052.	5.3	42

#	Article	IF	CITATIONS
37	Multidetector Computed Tomography in Reperfused Acute Myocardial Infarction. Investigative Radiology, 2008, 43, 773-781.	6.2	41
38	No post-conditioning in the human heart with thrombolysis in myocardial infarction flow 2-3 on admission. European Heart Journal, 2014, 35, 1675-1682.	2.2	41
39	Comparison of strain imaging techniques in CRT candidates: CMR tagging, CMR feature tracking and speckle tracking echocardiography. International Journal of Cardiovascular Imaging, 2018, 34, 443-456.	1.5	38
40	Gadobutrol-Enhanced Cardiac Magnetic Resonance Imaging for Detection of Coronary Artery Disease. Journal of the American College of Cardiology, 2020, 76, 1536-1547.	2.8	38
41	Free-Breathing Diffusion Tensor Imaging and Tractography of the Human Heart in Healthy Volunteers Using Wavelet-Based Image Fusion. IEEE Transactions on Medical Imaging, 2015, 34, 306-316.	8.9	37
42	Comparison of the angiographic myocardial blush grade with delayedâ€enhanced cardiac magnetic resonance for the assessment of microvascular obstruction in acute myocardial infarctions. Catheterization and Cardiovascular Interventions, 2009, 74, 1000-1007.	1.7	36
43	Headâ€ŧoâ€head comparison of eight late gadoliniumâ€enhanced cardiac MR (LGE CMR) sequences at 1.5 tesla: From bench to bedside. Journal of Magnetic Resonance Imaging, 2011, 34, 1374-1387.	3.4	35
44	Feature-based interpolation of diffusion tensor fields and application to human cardiac DT-MRI. Medical Image Analysis, 2012, 16, 459-481.	11.6	34
45	Churg–Strauss Syndrome Presenting with Acute Myocarditis and Cardiogenic Shock. Heart Lung and Circulation, 2012, 21, 178-181.	0.4	33
46	Comparison of regularization methods for human cardiac diffusion tensor MRI. Medical Image Analysis, 2009, 13, 405-418.	11.6	32
47	Statistical Analysis of the Human Cardiac Fiber Architecture from DT-MRI. Lecture Notes in Computer Science, 2011, , 171-179.	1.3	31
48	Lung Perfusion Demonstrated by Contrast-Enhanced Dynamic Magnetic Resonance Imaging. Investigative Radiology, 1997, 32, 351-356.	6.2	31
49	TypeÂ2 diabetes mellitus and obesity in young adults: the extreme phenotype with early cardiovascular dysfunction. Diabetic Medicine, 2014, 31, 794-798.	2.3	30
50	Adaptive Postprocessing Techniques for Myocardial Tissue Tracking with Displacement-encoded MR Imaging. Radiology, 2008, 246, 229-240.	7.3	29
51	Presence and Extent of Cardiac Magnetic Resonance Microvascular Obstruction in Reperfused Non-ST-Elevated Myocardial Infarction and Correlation with Infarct Size and Myocardial Enzyme Release. Cardiology, 2009, 113, 50-58.	1.4	28
52	Comparison of visual scoring and quantitative planimetry methods for estimation of global infarct size on delayed enhanced cardiac MRI and validation with myocardial enzymes. European Journal of Radiology, 2011, 78, 87-92.	2.6	28
53	Magnetic resonance imaging assessment of intraventricular dyssynchrony and delayed enhancement as predictors of response to cardiac resynchronization therapy in patients with heart failure of ischaemic and non-ischaemic etiologies. European Journal of Radiology, 2012, 81, 2639-2647.	2.6	28
54	Myocardial biomarkers and delayed enhanced cardiac magnetic resonance relationship in clinically suspected myocarditis and insight on clinical outcome. Journal of Cardiovascular Medicine, 2015, 16, 696.	1.5	28

#	Article	IF	CITATIONS
55	Exploratory analysis of the spatio-temporal deformation of the myocardium during systole from tagged MRI. IEEE Transactions on Biomedical Engineering, 2002, 49, 1328-1339.	4.2	27
56	Muscarinic Receptor Upregulation in Patients With Myocardial Infarction. Circulation: Cardiovascular Imaging, 2009, 2, 365-372.	2.6	27
57	PCATMIP: Enhancing signal intensity in diffusionâ€weighted magnetic resonance imaging. Magnetic Resonance in Medicine, 2011, 65, 1611-1619.	3.0	27
58	Assessment of complicated arterial bypass grafts: Value of contrast-enhanced subtraction magnetic resonance angiography. Journal of Vascular Surgery, 1997, 26, 1036-1042.	1.1	25
59	Precision of myocardial contour estimation from tagged MR images with a "black-blood―technique. Academic Radiology, 1998, 5, 93-100.	2.5	24
60	A FEM-based deformable model for the 3D segmentation and tracking of the heart in cardiac MRI. , 0, , .		24
61	Strain imaging to predict response to cardiac resynchronization therapy: a systematic comparison of strain parameters using multiple imaging techniques. ESC Heart Failure, 2018, 5, 1130-1140.	3.1	24
62	Cine and tagged cardiovascular magnetic resonance imaging in normal rat at 1.5 T: a rest and stress study. Journal of Cardiovascular Magnetic Resonance, 2008, 10, 48.	3.3	23
63	Left Ventricular Postmyocardial Infarction Remodeling Studied by Combining MR-Tagging With Delayed MR Contrast Enhancement. Investigative Radiology, 2008, 43, 219-228.	6.2	23
64	T1 mapping performance and measurement repeatability: results from the multi-national T1 mapping standardization phantom program (T1MES). Journal of Cardiovascular Magnetic Resonance, 2020, 22, 31.	3.3	23
65	A graphâ€based approach for automatic cardiac tractography. Magnetic Resonance in Medicine, 2010, 64, 1215-1229.	3.0	22
66	T2â€weighted cardiac MR assessment of the myocardial areaâ€atâ€risk and salvage area in acute reperfused myocardial infarction: Comparison of stateâ€ofâ€theâ€art dark blood and bright blood T2â€weighted sequences. Journal of Magnetic Resonance Imaging, 2012, 35, 328-339.	3.4	22
67	Assessment of Cardiac Motion Effects on the Fiber Architecture of the Human Heart In Vivo. IEEE Transactions on Medical Imaging, 2013, 32, 1928-1938.	8.9	22
68	Comparison of local sine wave modeling with harmonic phase analysis for the assessment of myocardial strain. Journal of Magnetic Resonance Imaging, 2013, 38, 320-328.	3.4	22
69	Relationship Between Ascending Thoracic Aortic Aneurysms Hemodynamics and Biomechanical Properties. IEEE Transactions on Biomedical Engineering, 2020, 67, 949-956.	4.2	22
70	Coupling hemodynamics with mechanobiology in patient-specific computational models of ascending thoracic aortic aneurysms. Computer Methods and Programs in Biomedicine, 2021, 205, 106107.	4.7	21
71	Denoising human cardiac diffusion tensor magnetic resonance images using sparse representation combined with segmentation. Physics in Medicine and Biology, 2009, 54, 1435-1456.	3.0	20
72	Characterization of normal regional myocardial function by MRI cardiac tagging. Journal of Magnetic Resonance Imaging, 2015, 41, 83-92.	3.4	20

#	Article	IF	CITATIONS
73	A new look at left ventricular remodeling definition by cardiac imaging. International Journal of Cardiology, 2016, 209, 17-19.	1.7	20
74	Strain analysis is superior to wall thickening in discriminating between infarcted myocardium with and without microvascular obstruction. European Radiology, 2018, 28, 5171-5181.	4.5	20
75	Role of upfront CT pulmonary angiography at admission in COVID-19 patients. Thrombosis Research, 2020, 196, 138-140.	1.7	20
76	Mechanisms leading to reversible mechanical dysfunction in severe CAD: alternatives to myocardial stunning. American Journal of Physiology - Heart and Circulatory Physiology, 2006, 291, H2570-H2582.	3.2	19
77	Influence of Microvascular Obstruction on Regional Myocardial Deformation in the Acute Phase of Myocardial Infarction: A Speckle-Tracking Echocardiography Study. Journal of the American Society of Echocardiography, 2014, 27, 93-100.	2.8	19
78	Pre-PCI angiographic TIMI flow in the culprit coronary artery influences infarct size and microvascular obstruction in STEMI patients. Journal of Cardiology, 2016, 67, 248-253.	1.9	18
79	MRI of Reperfused Acute Myocardial Infarction Edema: ADC Quantification versus T1 and T2 Mapping. Radiology, 2020, 295, 542-549.	7.3	18
80	Comparison between qualitative and quantitative wall motion analyses using dipyridamole stress breath-hold cine magnetic resonance imaging in patients with severe coronary artery stenosis. Magnetic Resonance Imaging, 1997, 15, 891-898.	1.8	17
81	Image-Based Investigation of Human in Vivo Myofibre Strain. IEEE Transactions on Medical Imaging, 2016, 35, 2486-2496.	8.9	17
82	Ascending thoracic aorta aneurysm repair induces positive hemodynamic outcomes in a patient with unchanged bicuspid aortic valve. Journal of Biomechanics, 2018, 81, 145-148.	2.1	17
83	Extreme Mountain Ultra-Marathon Leads to Acute but Transient Increase in Cerebral Water Diffusivity and Plasma Biomarkers Levels Changes. Frontiers in Physiology, 2017, 7, 664.	2.8	16
84	Expanding the cardiac spectrum of Noonan syndrome with RIT1 variant: Left main coronary artery atresia causing sudden death. European Journal of Medical Genetics, 2017, 60, 299-302.	1.3	15
85	Factor Analysis of Medical Image Sequences Improves Evaluation of First-Pass MR Imaging Acquisitions for Myocardial Perfusion. Academic Radiology, 2002, 9, 26-39.	2.5	14
86	Simulation based evaluation of cardiac motion estimation methods in tagged-MR Image sequences. Journal of Cardiovascular Magnetic Resonance, 2011, 13, .	3.3	14
87	Quantitative comparison of human myocardial fiber orientations derived from DTI and polarized light imaging. Physics in Medicine and Biology, 2018, 63, 215003.	3.0	14
88	Accuracy of right ventricular volume and function assessed with cardiovascular magnetic resonance: comparison with echocardiographic parameters. Clinical Imaging, 2020, 59, 61-67.	1.5	14
89	Giant coronary artery aneurysm mimicking a compressive cardiac tumor. Cardiovascular Pathology, 2005, 14, 272-275.	1.6	13
90	Cardioprotection in the Clinical Setting. Cardiovascular Drugs and Therapy, 2010, 24, 281-287.	2.6	13

#	Article	IF	CITATIONS
91	Cardiac Magnetic Resonance for Early Detection of Radiation Therapy-Induced Cardiotoxicity in a Small Animal Model. JACC: CardioOncology, 2021, 3, 113-130.	4.0	13
92	Interpolation of vector fields from human cardiac DT-MRI. Physics in Medicine and Biology, 2011, 56, 1415-1430.	3.0	12
93	Neprilysin levels at the acute phase of STâ€elevation myocardial infarction. Clinical Cardiology, 2019, 42, 32-38.	1.8	12
94	In vivo estimation of normal left ventricular stiffness and contractility based on routine cine MR acquisition. Medical Engineering and Physics, 2020, 85, 16-26.	1.7	12
95	Colchicine for Left Ventricular Infarct Size Reduction in Acute Myocardial Infarction: A Phase II, Multicenter, Randomized, Double-Blinded, Placebo-Controlled Study Protocol – The COVERT-MI Study. Cardiology, 2021, 146, 151-160.	1.4	12
96	Cardiovascular magnetic resonance tagging imaging correlates with myocardial dysfunction and T2 mapping in idiopathic dilated cardiomyopathy. International Journal of Cardiovascular Imaging, 2014, 30, 145-152.	1.5	11
97	Chemical-Shift-Encoded Magnetic Resonance Imaging and Spectroscopy to Reveal Immediate and Long-Term Multi-Organs Composition Changes of a 14-Days Periodic Fasting Intervention: A Technological and Case Report. Frontiers in Nutrition, 2019, 6, 5.	3.7	11
98	Reliability of standardized ultrasound measurements of quadriceps muscle thickness in neurological critically ill patients: a comparison to computed tomography measures Journal of Rehabilitation Medicine, 2020, 52, jrm00032.	1.1	11
99	Statistical Atlas of Human Cardiac Fibers: Comparison with Abnormal Hearts. Lecture Notes in Computer Science, 2012, , 207-213.	1.3	11
100	Dobutamine-tagged MRI for inotropic reserve assessment in severe CAD: relationship with PET findings. American Journal of Physiology - Heart and Circulatory Physiology, 2004, 286, H1946-H1953.	3.2	10
101	Quantification of Right and Left Ventricular Function in Cardiac MR Imaging: Comparison of Semiautomatic and Manual Segmentation Algorithms. Diagnostics, 2013, 3, 271-282.	2.6	10
102	A Comparative Study of Different Level Interpolations for Improving Spatial Resolution in Diffusion Tensor Imaging. IEEE Journal of Biomedical and Health Informatics, 2014, 18, 1317-1327.	6.3	10
103	Analytic signal phase-based myocardial motion estimation in tagged MRI sequences by a bilinear model and motion compensation. Medical Image Analysis, 2015, 24, 149-162.	11.6	10
104	Predictive value of early cardiac magnetic resonance imaging functional and geometric indexes for adverse left ventricular remodelling in patients with anterior ST-segment elevation myocardial infarction: A report from the CIRCUS study. Archives of Cardiovascular Diseases, 2020, 113, 710-720.	1.6	10
105	Myofiber strain in healthy humans using DENSE and cDTI. Magnetic Resonance in Medicine, 2021, 86, 277-292.	3.0	10
106	MR imaging of the heart: functional imaging. European Radiology, 2000, 10, 7-11.	4.5	9
107	MRI reconstruction from 2D truncated <i>k</i> â€space. Journal of Magnetic Resonance Imaging, 2012, 35, 1196-1206.	3.4	9
108	Quantification of left ventricular dyssynchrony in patients with systolic dysfunction: A comparison of circumferential strain MRâ€ŧagging metrics. Journal of Magnetic Resonance Imaging, 2014, 40, 1238-1246.	3.4	9

#	Article	IF	CITATIONS
109	Simultaneous strain–volume analysis by three-dimensional echocardiography. Journal of Cardiovascular Medicine, 2017, 18, 223-229.	1.5	9
110	A gradient-based optical-flow cardiac motion estimation method for cine and tagged MR images. Medical Image Analysis, 2019, 57, 136-148.	11.6	9
111	Computational prediction of hemodynamical and biomechanical alterations induced by aneurysm dilatation in patientâ€specific ascending thoracic aortas. International Journal for Numerical Methods in Biomedical Engineering, 2020, 36, e3326.	2.1	9
112	Usefulness of MRI to Demonstrate the Mechanisms of Myocardial Ischemia in Hypertrophic Cardiomyopathy with Myocardial Bridge. Cardiology, 2007, 107, 159-164.	1.4	8
113	Towards In Vivo Diffusion Tensor MRI on Human Heart using Edge-Preserving Regularization. Annual International Conference of the IEEE Engineering in Medicine and Biology Society, 2007, 2007, 6008-11.	0.5	8
114	Quantifying the effect of tissue deformation on diffusion-weighted MRI: a mathematical model and an efficient simulation framework applied to cardiac diffusion imaging. Physics in Medicine and Biology, 2016, 61, 5662-5686.	3.0	8
115	Estimation of cardiac motion in cine-MRI sequences by correlation transform optical flow of monogenic features distance. Physics in Medicine and Biology, 2016, 61, 8640-8663.	3.0	8
116	Effects of glycaemic variability on cardiac remodelling after reperfused myocardial infarction: Evaluation of streptozotocin-induced diabetic Wistar rats using cardiac magnetic resonance imaging. Diabetes and Metabolism, 2016, 42, 342-350.	2.9	8
117	Hemodynamics alteration in patient-specific dilated ascending thoracic aortas with tricuspid and bicuspid aortic valves. Journal of Biomechanics, 2020, 110, 109954.	2.1	8
118	Association of myocardial hemorrhage and persistent microvascular obstruction with circulating inflammatory biomarkers in STEMI patients. PLoS ONE, 2021, 16, e0245684.	2.5	8
119	Simultaneous myocardial strain and darkâ€blood perfusion imaging using a displacementâ€encoded MRI pulse sequence. Magnetic Resonance in Medicine, 2010, 64, 787-798.	3.0	7
120	Regional cardiac function analysis from tagged MRI images. Comparison of techniques: Harmonic-Phase (HARP) versus Sinusoidal-Modeling (SinMod) analysis. Magnetic Resonance Imaging, 2018, 54, 271-282.	1.8	7
121	Motionâ€Induced Signal Loss in In Vivo Cardiac Diffusionâ€Weighted Imaging. Journal of Magnetic Resonance Imaging, 2020, 51, 319-320.	3.4	7
122	Automatic Registration of MR First-Pass Myocardial Perfusion Images. Lecture Notes in Computer Science, 2003, , 215-223.	1.3	7
123	A Strategy to Quantitatively Evaluate MRI/PET Cardiac Rigid Registration Methods Using a Monte Carlo Simulator. Lecture Notes in Computer Science, 2003, , 194-204.	1.3	7
124	Quantitative Magnetic Resonance Imaging Assessment of the Quadriceps Changes during an Extreme Mountain Ultramarathon. Medicine and Science in Sports and Exercise, 2021, 53, 869-881.	0.4	7
125	Gender and Strain Variations in Left Ventricular Cardiac Function and Mass Determined With Magnetic Resonance Imaging at 7 Tesla in Adult Mice. Investigative Radiology, 2007, 42, 1-7.	6.2	6
126	The role of imaging and molecular imaging in the early detection of metabolic and cardiovascular dysfunctions. International Journal of Obesity, 2010, 34, S67-S81.	3.4	6

#	Article	IF	CITATIONS
127	Myocardial adaptation after surgical therapy differs for aortic valve stenosis and hypertrophic obstructive cardiomyopathy. International Journal of Cardiovascular Imaging, 2019, 35, 1089-1100.	1.5	6
128	Ventricular muscarinic receptor remodeling in patients with and without primary ventricular fibrillation. An imaging study. Journal of Nuclear Cardiology, 2012, 19, 1017-1025.	2.1	5
129	CMRSegTools: an Osirix plugin for myocardial infarct sizing on DE-CMR images. Journal of Cardiovascular Magnetic Resonance, 2014, 16, P204.	3.3	5
130	Location of Hamstring Injuries Based on Magnetic Resonance Imaging: A Systematic Review. Sports Health, 2023, 15, 111-123.	2.7	5
131	Non-rigid motion-corrected free-breathing 3D myocardial Dixon LGE imaging in a clinical setting. European Radiology, 2022, 32, 4340-4351.	4.5	5
132	Myocardial perfusion and glucose uptake coupling in CAD patients. International Journal of Cardiovascular Imaging, 2003, 19, 389-399.	0.6	4
133	Improved image reconstruction incorporating non-rigid motion correction for cardiac MRI using BLADE acquisition. Journal of Cardiovascular Magnetic Resonance, 2009, 11, .	3.3	4
134	Strain analysis in CRT candidates using the novel segment length in cine (SLICE) post-processing technique on standard CMR cine images. European Radiology, 2017, 27, 5158-5168.	4.5	4
135	Interactive drawing of the left ventricular borders from cine magnetic resonance images. Magnetic Resonance Materials in Physics, Biology, and Medicine, 1994, 2, 13-20.	2.0	3
136	Why Delay Intervention in STEMI?. JACC: Cardiovascular Imaging, 2011, 4, 921-922.	5.3	3
137	A novel contribution towards coherent and reproducible intravalvular measurement of the aortic annulus by multidetector computed tomography ahead of transcatheter aortic valve implantation. Archives of Cardiovascular Diseases, 2015, 108, 281-292.	1.6	3
138	Comparison of 2D simultaneous multi-slice and 3D GRASE readout schemes for pseudo-continuous arterial spin labeling of cerebral perfusion at 3 T. Magnetic Resonance Materials in Physics, Biology, and Medicine, 2021, 34, 437-450.	2.0	3
139	Incorporating Low-Level Constraints for the Retrieval of Personalised Heart Models from Dynamic MRI. Lecture Notes in Computer Science, 2010, , 174-183.	1.3	3
140	Variability of the HumanÂCardiacÂLaminarÂStructure. Lecture Notes in Computer Science, 2012, , 160-167.	1.3	3
141	Hubless 3D Medical Image Bundle Registration. , 2016, , .		3
142	Kinetics of Cardiac Remodeling and Fibrosis Biomarkers During an Extreme Mountain Ultramarathon. Frontiers in Cardiovascular Medicine, 2022, 9, 790551.	2.4	3
143	Myocardial motion estimation using optical flow with multiple constraint equations. , 2014, , .		2
144	Assessment of myocardial partition coefficient of gadolinium (λ) in dilated cardiomyopathy and its impact on segmental and global systolic function. Journal of Magnetic Resonance Imaging, 2014, 40, 1336-1341.	3.4	2

#	Article	IF	CITATIONS
145	Reply. Journal of the American College of Cardiology, 2015, 65, 2358-2359.	2.8	2
146	In vivo free-breathing DTI & IVIM of the whole human heart using a real-time slice-followed SE-EPI navigator-based sequence: a reproducibility study in healthy volunteers. Journal of Cardiovascular Magnetic Resonance, 2015, 17, P383.	3.3	2
147	Strain-Based Parameters for Infarct Localization: Evaluation via a Learning Algorithm on a Synthetic Database of Pathological Hearts. Lecture Notes in Computer Science, 2017, , 106-114.	1.3	2
148	Subacute Coronary Artery Thrombosis: MRI Findings. Journal of Computer Assisted Tomography, 1997, 21, 962-964.	0.9	2
149	Noise-Reduced TPS Interpolation of Primary Vector Fields for Fiber Tracking in Human Cardiac DT-MRI. Lecture Notes in Computer Science, 2009, , 78-86.	1.3	2
150	Estimation de mouvement par décalage de phase et maillage déformable appliquée à des séquences cardiaques d'IRM marquées. Traitement Du Signal, 2011, 28, 643-663.	1.3	2
151	Estimation of In Vivo Myocardial Fibre Strain Using an Architectural Atlas of the Human Heart. Lecture Notes in Computer Science, 2013, , 208-215.	1.3	2
152	Automated Quantification of Myocardial Infarction Using a Hidden Markov Random Field Model and the EM Algorithm. Lecture Notes in Computer Science, 2015, , 256-264.	1.3	2
153	Validation of cardiac diffusion tensor imaging sequences: A multicentre test–retest phantom study. NMR in Biomedicine, 2022, 35, e4685.	2.8	2
154	Tagged MRI and PET in severe CAD: discrepancy between preoperative inotropic reserve and intramyocardial functional outcome after revascularization. American Journal of Physiology - Heart and Circulatory Physiology, 2004, 287, H2226-H2233.	3.2	1
155	Improved global cardiac tractography with simulated annealing. , 2009, , .		1
156	Multiple myocardial infarctions in a 35 year-old woman with POEMS syndrome. European Heart Journal, 2010, 31, 1097-1097.	2.2	1
157	Cine Displacement ENcoding imaging with Stimulated Echoes (cine-DENSE) confirms systolic myocardial dysfunction in asymptomatic patients with type 2 diabetes mellitus: comparison with MR-tagging. Journal of Cardiovascular Magnetic Resonance, 2011, 13, .	3.3	1
158	DT-MRI interpolation: At what level?. , 2012, , .		1
159	T2-Weighted CMR. JACC: Cardiovascular Imaging, 2012, 5, 233-234.	5.3	1
160	Cardiac imaging research group. Results and future works. Irbm, 2013, 34, 21-23.	5.6	1
161	Multimodal quantification and validation of 3D regional myocardial function. Irbm, 2015, 36, 70-79.	5.6	1
162	Prediction of recovery after revascularization in chronic Coronary Total Occlusion (CTO) patients. Adenosine or low-dose dobutamine stress with LGE CMR: which is the best combination?. Journal of Cardiovascular Magnetic Resonance, 2015, 17, .	3.3	1

#	Article	IF	CITATIONS
163	In vivo freeâ€breathing DTI and IVIM of the whole human heart using a realâ€time sliceâ€followed SEâ€EPI navigatorâ€based sequence: A reproducibility study in healthy volunteers. Magnetic Resonance in Medicine, 2016, 76, spcone.	3.0	1
164	Automatic myocardial ischemic lesion detection on magnetic resonance perfusion weighted imaging prior perfusion quantification: A pre-modeling strategy. Computers in Biology and Medicine, 2019, 110, 108-119.	7.0	1
165	Regional myocardial function at preclinical disease stage of hypertrophic cardiomyopathy in female gene variant carriers. International Journal of Cardiovascular Imaging, 2021, 37, 2001-2010.	1.5	1
166	Direct Comparison of Bayesian and Fermi Deconvolution Approaches for Myocardial Blood Flow Quantification: In silico and Clinical Validations. Frontiers in Physiology, 2021, 12, 483714.	2.8	1
167	Significance of Hemodynamics Biomarkers, Tissue Biomechanics and Numerical Simulations in the Pathogenesis of Ascending Thoracic Aortic Aneurysms. Current Pharmaceutical Design, 2021, 27, 1890-1898.	1.9	1
168	Cardiac Fibre Trace Clustering for the Interpretation of the Human Heart Architecture. Lecture Notes in Computer Science, 2009, , 39-48.	1.3	1
169	Comparison of Different Strain-Based Parameters to Identify Human Left Ventricular Myocardial Infarct During Diastole: A 3D Finite-Element Study. Lecture Notes in Bioengineering, 2018, , 161-169.	0.4	1
170	Characterizing Myocardial Ischemia and Reperfusion Patterns with Hierarchical Manifold Learning. Lecture Notes in Computer Science, 2022, , 66-74.	1.3	1
171	An Adaptive Denoising Method Dedicated to Cardiac MR-DTI. , 2009, , .		Ο
172	Determination of the myocardial area at risk after reperfused acute myocardial infarction with different imaging techniques: cardiac magnetic resonance imaging, multidetector computed tomography and histopathological validation. Journal of Cardiovascular Magnetic Resonance, 2011, 13,	3.3	0
173	Potential of pre-contrast T1 mapping as a marker of interstitial fibrosis in severe aortic stenosis. Journal of Cardiovascular Magnetic Resonance, 2012, 14, .	3.3	0
174	Maximum energy tracking approach to reconstructing human cardiac fibers from DTI. , 2014, , .		0
175	Myocardial Salvage, Area at Risk by T2w CMR. Journal of the American College of Cardiology, 2015, 65, 2357-2358.	2.8	0
176	Apparent Diffusion coefficient (ADC), T1 and T2 quantitative indexes of the myocardium in athletes before, during and after extreme mountain ultra-marathon: correlation with myocardial damages and inflammation biomarkers. Journal of Cardiovascular Magnetic Resonance, 2016, 18, O41.	3.3	0
177	Comparison of three diffusion encoding schemes for cardiac imaging under free breathing conditions Journal of Cardiovascular Magnetic Resonance, 2016, 18, W16.	3.3	0
178	Does T1-mapping in border-zone and/or remote regions can help to predict functional recovery after revascularization in chronic Coronary Total Occlusion (CTO) patients?. Journal of Cardiovascular Magnetic Resonance, 2016, 18, O45.	3.3	0
179	IMPACT OF AN ULTRA-MARATHON OF 330 KM ON PLASMA LEVELS OF CARDIAC BIOMARKERS. British Journal of Sports Medicine, 2017, 51, 348.1-348.	6.7	0
180	Letter by Mewton and Croisille Regarding Article, "ldentification of High-Risk Patients After ST-Segment–Elevation Myocardial Infarction: Comparison Between Angiographic and Magnetic Resonance Parameters― Circulation: Cardiovascular Imaging, 2017, 10, .	2.6	0

#	Article	IF	CITATIONS
181	Potential of Low Energy UltraSound for Inducing Cardioprotection Mechanisms: In-Vitro Investigations on a Hypoxia-Reoxygenation Model of Cardiac Cells. , 2018, , .		Ο
182	Impact of Distortion on Local Radiomic Analysis of Quadriceps Based on Quantitative Magnetic Resonance Imaging Data. International Journal of Pharma Medicine and Biological Sciences, 2021, 10, 49-54.	0.2	0
183	Nonculprit Artery Myocardial Infarction and Complex Coronary Lesions in Anterior ST-Elevated Myocardial Infarction Patients: Data from the CIRCUS Study. Cardiology, 2021, 146, 728-736.	1.4	0
184	Driving Dynamic Cardiac Model Adaptation with MR-Tagging Displacement Information. Lecture Notes in Computer Science, 2011, , 137-144.	1.3	0
185	Comparison of Dobutamine Stress Tagged MRI With F-18 FDG PET to Assess Myocardial Viability in Patients With Chronic Ischemic Heart Disease. Journal of the American College of Cardiology, 1998, 31, 384A.	2.8	0
186	297â€Cardiac fibrosis markers: galectin-3 and suppression of tumorigenicity 2 measurement in participant at the Tor des Géants. , 2021, , .		0